3. Numerical Modelling

This chapter describes how numerical modelling was used in order to support and verify the conceptual hydrogeochemical model developed in the previous Sections, and to obtain further insight into the regional physical and geochemical processes occurring in the Chaudière-Appalaches region.

To date, the only existing modelling study within the Chaudière-Appalaches region was performed by Brun Koné (2013) (see also the corresponding GSC Report of Benoît et al. 2015) who developed a 3-D groundwater flow model for the Chaudière River watershed in order to estimate the impact of changes in recharge and water demand on the water table position. Using a maximum model depth of 300 meters, including shallow unconsolidated sediments and the fractured sedimentary rock, this model showed that most groundwater flow is focussed in the shallow rock. However, the model did not investigate deep regional flow. Additional groundwater flow models in two and three dimensions focusing on flow systems through shallow fractured rock have also been developed for other regions in Québec (Basses-Laurentides: Nastev et al. 2005; Châteauguay: Lavigne et al. 2010; Montérégie Est: Laurencelle et al. 2013; Outaouais: Montcoudiol et al. 2017; Saint-Charles River wastershed: Cochand 2014; Graf 2015). Although important insight was gained through these studies, the importance and role of deep regional flow in these flow systems remains to be defined.

The numerical model presented herein is specifically aimed at better understanding the relationships between local and regional flow systems within the Chaudière-Appalaches region with an emphasis on regional flow and groundwater discharge zones. Furthermore, this study aims at identifying how the main geologic features may influence the behaviour of regional flow. In particular, the study area is marked by the presence of major faults with uncertain hydraulic characteristics and which are presumed to be located within a regional flow discharge zone. A better understanding of the role of faults in regional and deep groundwater flow is particularly important regarding the risk to shallow groundwater quality from development of unconventional hydrocarbons (Lefebvre 2017; Rivard et al. 2014). This issue is of concern in the northern area of the CA study area, in which the Utica Shale is a prospective shale gas play (Lavoie et al. 2014).

Numerical modelling is used here to investigate the role of these faults on groundwater discharge. While the role of a conduit-type fault has been investigated for a generic regional basin with a geologic context comparable to the St. Lawrence Platform (Gassiat et al. 2013), the hydraulic behaviour of fault zones in the Chaudière study area has yet to be characterised (the work carried out by the Geological Survey of Canada was only partly released when the present study was undertaken; Ladevèze et al. 2015 and Ladevèze 2017); this knowledge gap will be addressed herein through numerical modelling.

3.1 Modelling Strategy

Numerical groundwater models should be used not as a final product or for absolute predictions but rather as tools to gain further understanding of a system (Voss 2011). In this context, a groundwater system should thus be represented in its simplest possible form while capturing it's most important behaviour (Voss 2011). In order to best capture the dynamics of regional flow in the Chaudière-Appalaches region, a two-dimensional groundwater flow model was developed following a regional flow path (Figures 2, 5 and 6), which was then coupled to an advective-dispersive age transport model. The flow and age transport simulations were completed using the finite element code FLONET/TR2 (Molson and Frind, 2017).

In FLONET/TR2, the two-dimensional steady-state groundwater flow equations are defined as a both a function of hydraulic heads (Equation 8) and stream functions (Equation 9) (Molson and Frind, 2017) :

$$\frac{\partial}{\partial x}\left(K_{xx}\frac{\partial \phi}{\partial x}\right)+\frac{\partial}{\partial y}\left(K_{yy}\frac{\partial \phi}{\partial y}\right)=0 \qquad (8)$$

$$\frac{\partial}{\partial x}\left(\frac{1}{K_{yy}}\frac{\partial \psi}{\partial x}\right)+\frac{\partial}{\partial y}\left(\frac{1}{K_{xx}}\frac{\partial \psi}{\partial y}\right)=0 \qquad (9)$$

Where,

x and y are the horizontal and vertical coordinate directions, respectively (L);

K_{xx} and K_{yy} are the principal components of the hydraulic conductivity tensor (L/T);

ϕ is the hydraulic head (L);

ψ is the stream function (L^2/T).

The steady-state saturated flow model was calibrated using PEST version 13.6 (Doherty 2015), a model-independent parameter estimation code. A sensitivity analysis was also performed in order to provide a deeper understanding of the influence of the selected parameters on the modelling outcome. The calibrated flow model was then used to simulate the transport of age mass. Finally, a parametric study on the role of faults was performed in order to investigate their potential influence on groundwater flowpaths.

3.2 Domain description

The domain represented by the numerical model corresponds to a two-dimensional projection of the conceptual groundwater flow model presented in Section 2.4 and corresponds to the geologic cross-Section presented in Section 2.1. The model follows an inferred regional flow path which extends from a local peak elevation in the Appalachian Highlands to the St. Lawrence River. In order to optimally capture the regional flow pattern, the modeled cross-Section is 69 km long with a maximum depth of 9.1 km. Three distinct geological provinces are included in the model: the Grenville crystalline bedrock, relatively flat-lying units of the sedimentary St. Lawrence Platform and the structurally complex and metamorphosed deep oceanic units of the Appalachians that are thrusted over the St. Lawrence Platform. The entire domain is covered by a discontinuous layer of surficial deposits of marine and glacial or fluvioglacial origins.

3.3 Steady-State Regional Flow Model

3.3.1 Assumptions and limitations

Several assumptions have been made in order to simplify the Chaudière-Appalaches model and reduce over-parameterization. First, given the regional scale of the study, fractured rock is represented as an equivalent porous medium. Also, using a two-dimensional model assumes that groundwater flow is perfectly aligned with the cross-Section and thus transverse hydraulic and age gradients are neglected. Since the cross-Section is parallel to regional topographic and piezometric gradients, it is considered well representative of the regional flow direction.

Furthermore, the flow system is simulated under steady-state conditions and thus does not account for seasonal (or climatic) variations of the recharge. Transient recharge is expected to have most impact on the local flow systems, with little or no significant impact on regional flow. Furthermore, water table fluctuations induced by seasonal recharge variations are also expected to be negligible with respect to inherent uncertainty, including the errors associated with the extrapolation of the regional potentiometric map, which is assumed to represent an annual average water level. Variations over geological time (ex. ice advances and retreats) are also neglected.

Moreover, the model assumes that groundwater in the domain has a uniform temperature, viscosity and density. The average thermal gradient in the area is between 15 and 20 ^{o}C/km (Grasby et al. 2011) which, based on an estimate of the Rayleigh number for average conditions found in the study area, is not sufficient for the onset of thermal convection (Hiscock and Bense 2014). Also, although measured TDS concentrations in the study area reach up to 16,785 mg/L (Bordeleau et al. 2017) and up to 340,000 mg/L in the deep formations of the St. Lawrence Platform (Ngoc et al. 2014), the effects of density and viscosity gradients on flow are assumed negligible relative to the logarithmic decrease with depth of the hydraulic conductivities (documented in Section 3.2.2.2).

3.3.2 Model Parameters

3.3.2.1 Domain Extent and Discretization

The estimated initial top boundary elevation of the model, representing the water table, was extracted from the regional potentiometric map (Lefebvre et al. 2015), while the elevations of the bedrock interface and the nine distinct surficial deposit layers were obtained from a detailed cross-Section of surficial deposits traced roughly along the modeled Section (Lefebvre et al. 2015). For modelling purposes, the rock formations within the cross-Section were divided into five different zones representing different rock types: the St. Lawrence Platform, the Appalachian Highlands, the Utica Shale, the carbonate platform and the Grenville formation.

The finite element flow model is discretized using linear triangular elements with a horizontal discretization of 50 m and a vertical discretization between 0.1 and 50 m (increasing from top to bottom), for a total of 358,000 nodes and 797,640 elements.

3.3.2.2 Material Properties

Material properties represented by the model can be classified as surficial deposits, the fractured bedrock aquifer and deep units.

Surficial deposits

Surficial deposits along the cross-Section are composed of nine different hydrostratigraphic units (Lefebvre et al. 2015): organic deposits, alluvium, lakeshore delta sediments, glaciomarine delta deposits, coarse and fine-grained littoral glaciomarine deposits, fluvio-glacial deposits, till and undifferentiated sand (Section 2.1). Each unit is represented by a layer of deformed elements in the model (Table 3). All layers of the surficial deposits were assumed to have an average porosity of 0.3.

Till is the most prominent unit over the study area and it is thus expected that its hydraulic conductivity will control groundwater flux reaching the fractured rock aquifer. The till unit also has the most heterogeneous composition; typically very sandy in the area of the cross-Section, its texture can vary abruptly from a permeable sand facies with a few pebbles to an essentially impermeable stony and clayey silt (G. Légaré Couture, personal communication 2013). Uncertainty with respect to the hydraulic conductivity of the till layer is addressed through calibration and sensitivity analysis.

Table 3 Physical description of the surficial deposits, including reported and calibrated hydraulic conductivities.

Mod. Unit	Geologic Group /Description	Hydraulic Description	Log K (m/s)			Reference	Calibrated log K (m/s)
org	Organic deposits (phagnum and ericaceous peat)	Poorly drained		-4.52		Tecsult (2008)	-4.73
				-5.00		Brun Koné (2013)	
				-6.48		Ladevèze (2015)	
all	Alluvium (silt and sand)	permeable		-4.00		Tecsult (2008)	-6.00
			-6.00	to	-3.00	Brun Koné (2013)	
			-7.44	to	-4.06	Ladevèze (2015)	
			-9.00	to	-4.70	Domenico and Schwartz (1998)	
lgd	Lakeshore delta (Sand, silts, gravel)	permeable	-6.00	to	-3.00	Brun Koné (2013)	-6.00
			-6.70	to	-3.52	Domenico and Schwartz (1998)	
mgd	Glaciomarine delta (Sand, silts, gravel)	permeable	-6.00	to	-3.00	Brun Koné (2013)	-5.9
			-6.70	to	-3.52	Domenico and Schwartz (1998)	
mgbg	Littoral glaciomarine (coarse) (Gravel, sand, silts)	permeable		-4.00		Tecsult (2008)	-4.4
			-6.00	to	-3.00	Brun Koné (2013)	
			-8.12	to	-5.27	Ladevèze (2015)	
			-6.70	to	-3.52	Domenico and Schwartz (1998)	
mgbf	Littoral glaciomarine (fine) (Silts, sand, gravel)	relatively permeable		-4.00		Tecsult (2008)	-5.97
			-6.00	to	-3.00	Brun Koné (2013)	
			-8.12	to	-5.27	Ladevèze (2015)	
			-6.70	to	-3.52	Domenico and Schwartz (1998)	
grav	Glaical/fluvioglacial (sand and gravel)	very permeable		-3.52		Tecsult (2008)	-3.96
			-6.00	to	-3.00	Brun Koné (2013)	
			-6.70	to	-3.52	Domenico and Schwartz (1998)	
till	Glacial tills (sand,silt, clay)	spatially variable		-8.52		Tecsult (2008)	-6.05
				-8.70		Tecsult (2008)	
				-6.22		Brun Koné (2013)	
			-12.00	to	-5.70	Domenico and Schwartz (1998)	
sab	Sand	permeable		-6.52		Tecsult (2008)	-4.86
				-7.00		Brun Koné (2013)	
			-9.00	to	-5.00	Ladevèze (2015)	
			-8.10	to	-3.52	Domenico and Schwartz (1998)	

Fractured bedrock

Hydraulic conductivities of the bedrock were obtained through the updated PACES-Chaudière-Appalaches database (Lefebvre et al. 2015) in which the extensive public well drillers' log data was used to estimate hydraulic conductivities (Figure 19). These data originate from specific capacity data while accounting for drilling and testing biases (M. Laurencelle, personal communication, June-July 2015; Lefebvre et al. 2015). Calculated hydraulic conductivities in the shallow bedrock (within the top 100 meters of the rock surface) are between 3.8×10^{-10} and 6.5×10^{-4} m/s in the St. Lawrence Platform (241 data points) and between 5.2×10^{-12} and 3.8×10^{-3} m/s in the Appalachian Highlands (4966 data points). Although the hydraulic conductivity of the bedrock is highly variable for a given depth, spanning more than 6 orders of magnitude, a clear trend of decreasing hydraulic conductivity with depth can be observed for both geologic provinces (Figure 19) (Lefebvre et al. 2015). The model hydraulic conductivities were calibrated by adjusting the parameters of an exponential decay function given by Equation 10:

$$\log[(K(z)] = log[K_{min}] - (log[K_{max}] - log[K_{min}])e^{-\alpha z} \qquad (10)$$

where :

z (m) is the depth below the top of the bedrock surface

K(z) is the hydraulic conductivity at depth z

K_{min} is the minimum hydraulic conductivity asymptotically approached by the curve

K_{max} is the maximum hydraulic conductivity, and

α is a curve decay constant

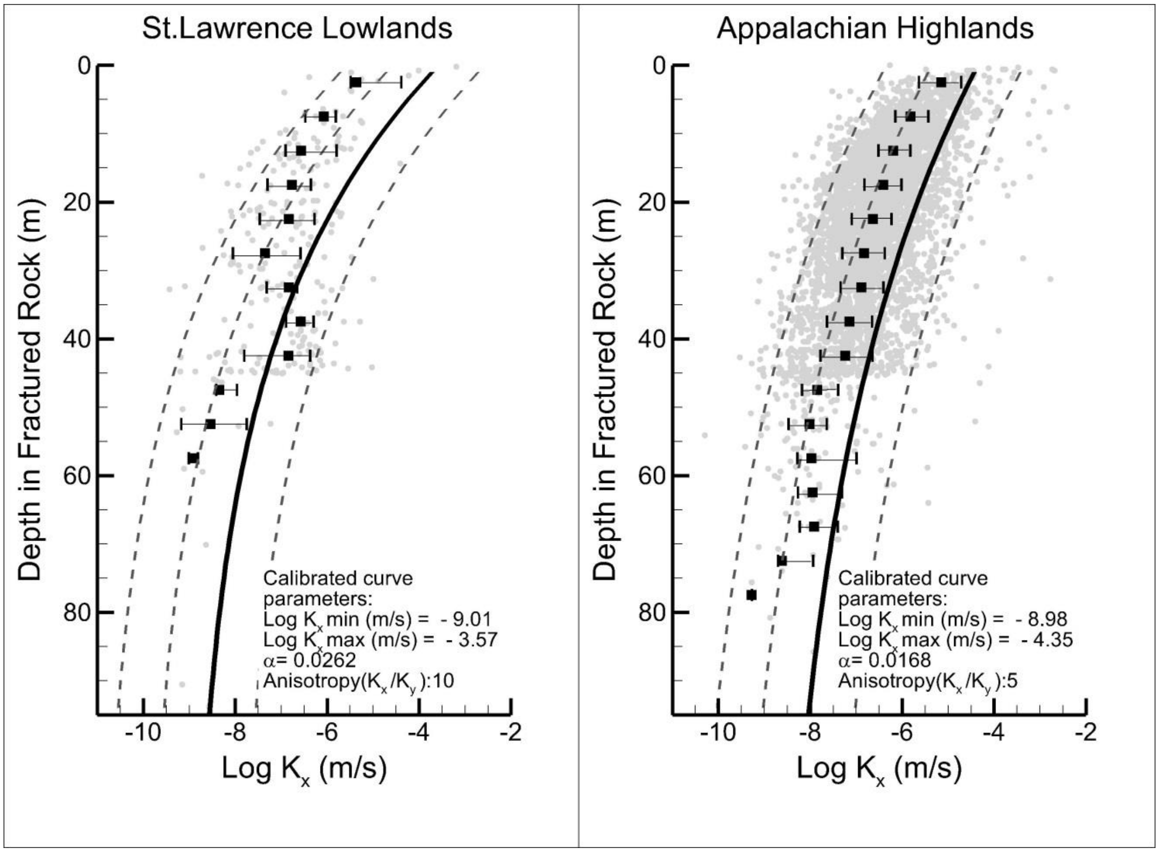

Figure 19 Distribution of hydraulic conductivities in Chaudière-Appalaches region. Grey dots represent measured data from the well drillers' log (Lefebvre et al. 2015). Black squares show the median measured value per 5 meter slices and the horizontal whiskers show the 25th and 75th percentiles. Solid lines show the calibrated distribution of hydraulic conductivities in the fractured bedrock and dotted lines show different conductivity scenarios tested in the sensitivity analysis.

Deep layers

The Grenville basement rock, the St. Lawrence Carbonate platform and the Utica Shale are described in the literature as having distinct hydraulic properties (Table 4; Section 2.1). In the model, these units are differentiated from the top fractured unit of the St. Lawrence Platform (Lorraine formation) and the Appalachian Highland formations. Conductivities assigned to these deep formations are described in Table 4.

Table 4 Description of the modeled geologic units, including the reported and modeled hydraulic conductivities and porosities (includes properties reported by Gassiat et al. 2013).

Model Unit	Geologic Group	Literature Description	log K (m/s) min to max	Por. (%)	Reference
Above Shale in SLP	Lorraine	Fine grained sedimentary[a]	-10.21 to -6.71		Gleeson et al. (2011)
	silty shales with mostly non calcareous	Lorraine unit matrix Bécancour (eastern Canada)[a,b]	-10.61	3.9	Tran Ngoc et al. (2014)
	sediments interbedded with fine	Fractured rock[c]	-6.47 to -4.96		Ladevèze (2015) Personal communication
	sandstone and clayey siltstones	Fractured rock in St. Lawrence Platform formation	-9.43 to -3.19		Lefebvre et al. (2015)
		Minimum values in model (log Kx/log Kz)	**-9.01/-10.01**	**5**	
Above Shale in AH	Humber zone	Fractured rock	-8.96 to -5.39		Ladevèze (2015) Personal communication
	carbonates, sandstones and shales	Fractured rock in Humber formation	-11.28 to -2.03		Lefebvre et al. (2015)
		Minimum values in model (log Kx/log Kz)	**-8.98/-9.68**	**5**	
Utica Shale	Utica shale	General[a]	-15.21 to -9.21		Neuzil (1994)
	calcareous black hale	General[a]	-12.21 to -8.21		Freeze and Cherry (1979)
		General[a]	-15.21 to -12.21		Flewelling and Sharma (2013)
		Utica (eastern Canada)[a]	-14.26 to -8.31		Séjouné et al. (2005)
		Marcellus (Northeastern USA)	-7.91		Soeder (1988)
		Barnett	-9.21		Montgomery et al.(2005)
		Utica unit Bécancour matrix (eastern Canada)[a,b]	-10.73	4	Tran Ngoc et al. (2014)
		log Kx/log Kz in model	**-9.5/-11.5**	**5**	
Carbonate Platform	Trenton	Trenton unit Bécancour matrix (eastern Canada)[a,b]	-7.81	3.4	Tran Ngoc et al. (2014)
	clayey limestone interbedded with shales	Trenton unit Bécancour global (eastern Canada)[a,b]	-5.10		Tran Ngoc et al. (2014)
	Black River	*limestone interbedded with sandstone*			
	Chazy	*clayey and sandy limestone*			
	Beakmantown	Beauharnois unit Bécancour matrix (eastern Canada)[a,b]	-8.26	1	Tran Ngoc et al. (2014)
	dolomitic sandstone becoming pure	Beauharnois unit Bécancour global (eastern Canada)[a,b]	-8.43		Tran Ngoc et al. (2014)
	dolostone then dolomic limestone	Theresa unit Bécancour matrix (eastern Canada)[a,b]	-8.43	2.6	Tran Ngoc et al. (2014)
		Theresa unit Bécancour global (eastern Canada)[a,b]	-8.10		Tran Ngoc et al. (2014)
	Potsdam	Cairnside unit Bécancour matrix (eastern Canada)[a,b]	-8.13	3.3	Tran Ngoc et al. (2014)
	poorly cemented sandstone formation	Cairnside unit Bécancour global (eastern Canada)[a,b]	-6.59		Tran Ngoc et al. (2014)
	becoming well cemented	Covey Hill unit Bécancour matrix (eastern Canada)[a,b]	-7.83	6.3	Tran Ngoc et al. (2014)
		Values in model	**-8/-9**	**1**	
Grenville	Grenville	Crystalline[a]	-9.21 to -4.71		Gleeson et al. (2011)
	unfractured metamorphic and igneous	Unfractured metamorphic and igneous rock	-12.21 to -8.71		Freeze and Cherry (1979)
		Calibrated hydraulic conductivities in Outaouais	-12 to -6.	1-3	Montcoudiol et al. (2017)
		log Kx/log Kz in model	**-11/-11**	**0.05**	

a- Calculated from permeability values using density = 1000 kg/m^3, viscosity = 8.90x10^{-4} Pa·s and g = 9.81 m/s^2, b- Median value given in study

3.3.2.2 Boundary conditions

Vertical boundaries, corresponding to the St. Lawrence River to the north-west and to a regional topographic and piezometric peak to the south-east, are assumed to represent symmetric physical boundaries of the flow system and were thus assigned a no-flow boundary condition. It is also assumed that no significant flow occurs below a depth of 9,100 m, thus a zero-flux condition was applied to the base of the model. At stream and river locations, the top boundary is constrained by imposed heads (Figure 20). Given that recharge is highly variable over the study area (Section 2.2), the top boundary was separated into 295 Sections; each with a unique recharge imposed as a Type-2 flux boundary condition which was determined with PEST during calibration.

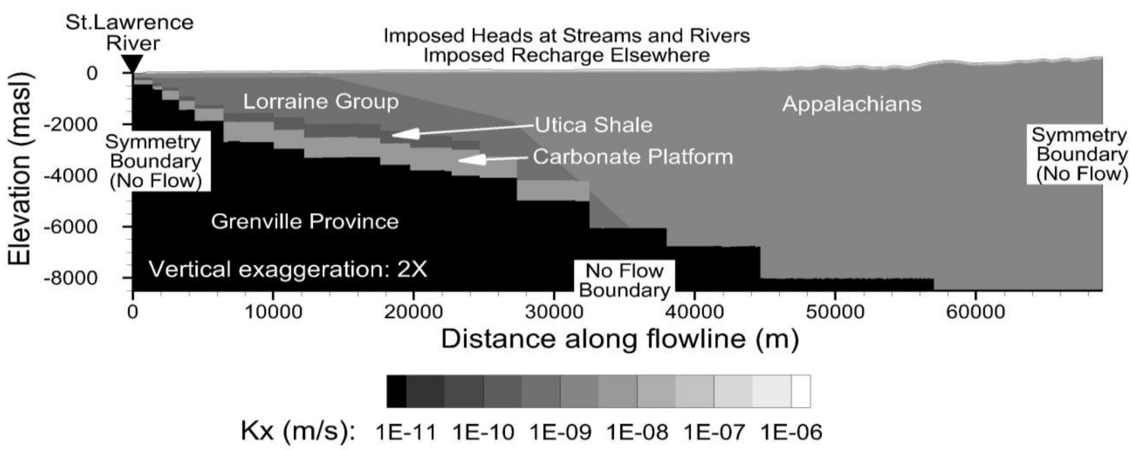

Figure 20 Geological structure, hydraulic conductivity and boundary conditions for the numerical flow model

3.3.3 Calibration

The numerical flow model was calibrated through a semi-automated workflow using PEST (version 13.6, Doherty 2015). PEST is a model-independent parameter estimation code which uses the Gauss-Levenberg-Marquardt search algorithm (GLMA) to minimize the difference between a set of observed (known) values and the corresponding simulated results (Doherty 2015). This software can be particularly useful when a large number of parameters need to be adjusted (calibrated) and when the relationship between the parameters and the observations is not linear (eg: Siade et al. 2015; Hayley et al. 2014; Zhu et al. 2015). Nevertheless, when field observations are not sufficient to appropriately constrain a model, calibration solutions will be non-unique and human input is needed to identify the most plausible solution. To this effect, PEST was used in this project to create many realisations of the flow model, each constraining the parameters of the model differently through various iterations of the parameter estimation. The realisation with the best fit to observation and the most plausible parameters was selected as the base case calibrated model.

Calibration was completed by coupling PEST to FLONET and allowing PEST to modify the hydraulic conductivities of each surficial deposit layer, as well as to define the decrease in hydraulic conductivity in the fractured bedrock using Equation 8, and to vary the imposed Type-2 Neumann recharge boundary condition for the 295 free water table Sections of the top boundary. Given the spatial variability in recharge calculated from one-dimensional infiltration models (Lefebvre et al. 2015; Benoît et al. 2014), recharge values imposed along the top boundary of the model were allowed to vary between 0 and 900 mm/year. The observations, to which PEST was trying to find the best fit, were taken to be the elevation of the water table at each of the top boundary nodes, and were extrapolated from a regional potentiometric map (Lefebvre et al. 2015). PEST was therefore trying to find the right parameter combination (K values and recharge), within defined ranges, which would result in simulated hydraulic heads best matching the regional piezometry. An additional verification step was performed which verified that the average recharge values imposed on the model by PEST were consistent with the values calculated from the one-dimensional infiltration model, HELP (Lefebvre et al. 2015; Benoît et al. 2014), based on the approach of Croteau et al. (2010).

With respect to the observed heads, which in the study area vary between 0 and over 600 m, the final calibrated model heads have an absolute mean error of 2.06 m, a root mean square error (RMSE) of 3.28 m and a maximum absolute error of 18.26 m (Figures 21 and 22). The error on modeled heads is well below 5% of the overall variations in heads in the model domain (30 m), which according to Anderson and Woessner (1992) defines the acceptability of a groundwater model hydraulic head calibration.

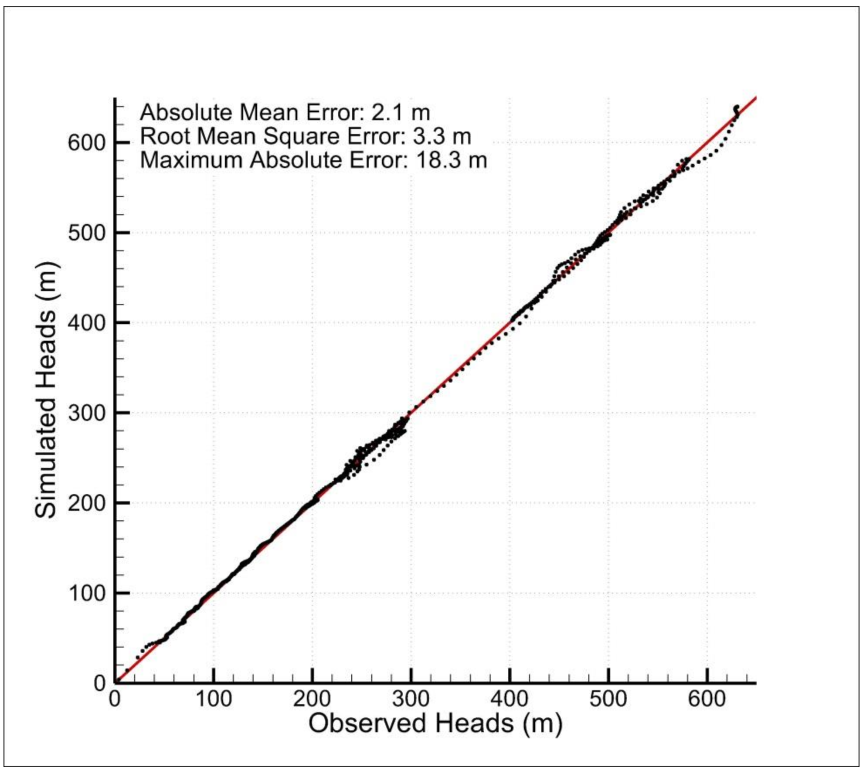

Figure 21 Model calibration: Observed heads (from interpolated regional piezometry) against simulated heads

The average overall calibrated recharge to the bedrock is within 1.04% of the average recharge estimated with the HELP model (Table 5). Moreover, despite some differences throughout the area between the model-calibrated average recharge to bedrock and the average values calculated with HELP, these calibrated recharge rates remain within the range of values estimated with HELP (Table 5). The model can therefore be considered as a fair representation of the natural groundwater system at the regional scale.

Table 5 Average recharge to the bedrock calibrated from the HELP model and from the current 2-D flow model (SLL = St. Lawrence Lowlands, AHL=Appalachian Highlands).

Average recharge to the bedrock	Modeled with HELP (Lefebvre et al. 2015)	Calibrated flow model	% Absolute Error
Overall (mm/year)	166	164	1.04
SLL (mm/year)	85 (<15 to >300)	63	25.64
AHL (mm/year)	187 (100 to >300)	326	74.27

Calibrated hydraulic conductivities of the surficial deposits are within the range of values found in the literature, with the exception of the till layer having a calibrated hydraulic conductivity slightly higher than reported (Table 3). The same phenomenon can be observed in the fractured bedrock hydraulic conductivity distribution (Figure 19); the calibrated hydraulic conductivity distribution for the fractured rock is approximately an order magnitude higher than the median hydraulic conductivities inferred from the well drillers' log data.

This discrepancy between measured and calibrated hydraulic conductivities can be attributed to the well-documented scaling effect (Schulze-Makuch et al. 1999; Zhang, Gable, and Person 2006; Nastev et al. 2004). Aquifers with heterogeneous properties or with fracture-controlled flow generally contain irregular areas of high and low permeability. The smaller the measurement volume of the hydraulic test performed in the aquifer, the less likely it is to intercept a preferential flow pathway such as interconnected fractures. Schulze-Makuch et al. (1999) observed that upscaling the radius of influence of hydraulic testing in a given heterogeneous aquifer could lead to an increase in measured hydraulic conductivity of up to one order of magnitude. This scale effect was also observed for fractured rock aquifers of the St. Lawrence Platform (Nastev et al. 2004).

In this study, hydraulic conductivities of the fractured bedrock (Figure 19) were mostly obtained from specific capacity tests for residential wells, which have a radius of influence of approximately 20 m (Nastev et al. 2004), while the groundwater flow model has a total length of 69,000 m with 50 m long elements. Given the difference in representation scale between the measured and calibrated hydraulic conductivities of the fractured bedrock, the calibrated model can be considered well representative of the fracture flow component occurring at the regional scale.

The scaling effect, which is explained by heterogeneities (Schulze-Makuch et al. 1999), also provides a rational to explain the calibrated hydraulic conductivities of till which are found at the higher end of the reported spectrum.

Sensitivity of the modelling results with respect to fractured bedrock and overburden hydraulic conductivities is further explored through a sensitivity analysis presented in Section 3.3.4.

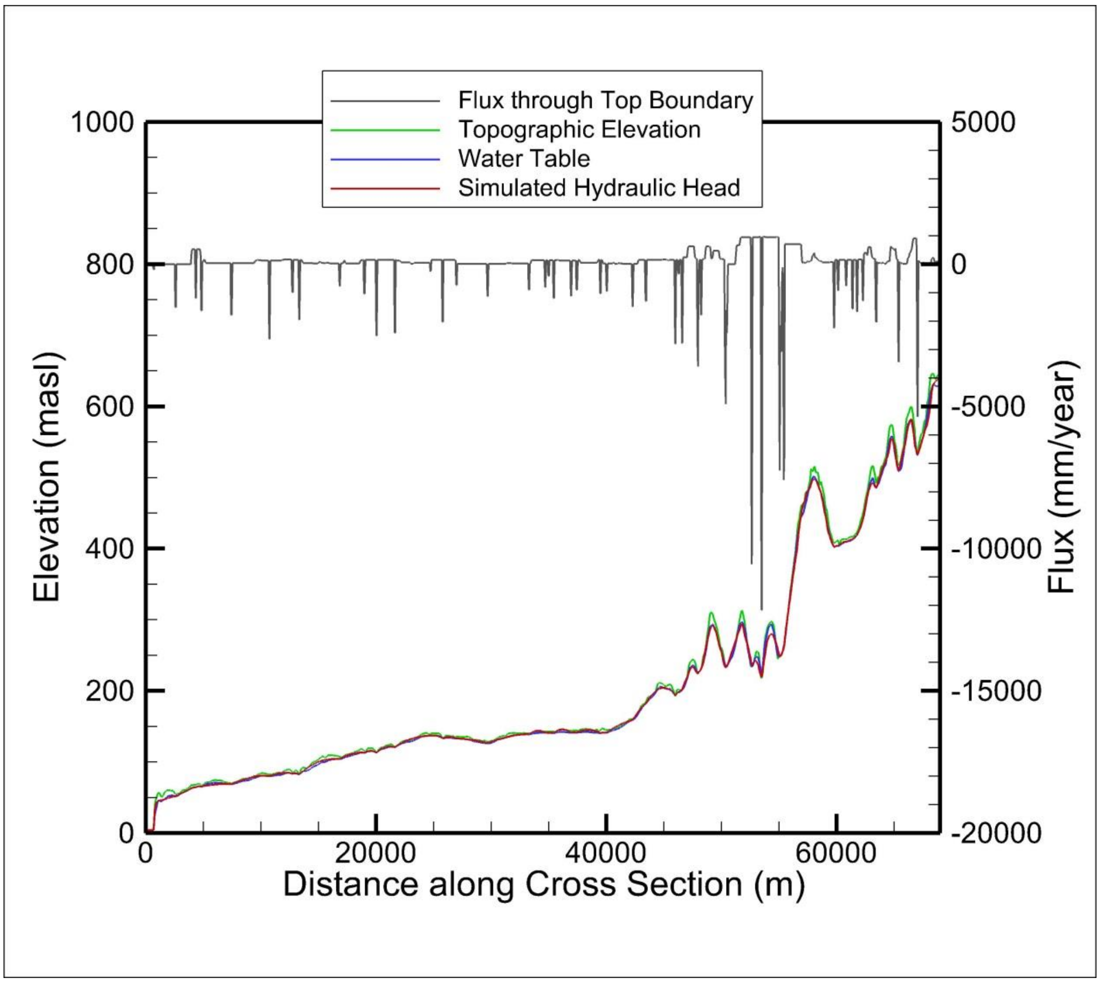

Figure 22 Calibrated recharge fluxes, simulated hydraulic heads, observed water table elevations (from interpolated piezometry) and topographic elevation along the model cross-Section. Negative fluxes are exiting the model domain and positive fluxes are entering

3.3.3 Flow Model Results

Figures 23 through 27 show the simulated potentiometric field and streamlines (flow lines) of the calibrated groundwater flow model. The model shows a clear Tóthian flow pattern with embedded regional, intermediate and local flow systems (Tóth 1999; Tóth 1963; Tóth 2009).

The simulated flow system is consistent with previous studies (Brun Koné 2013; Benoît et al. 2014) showing the dominance of local groundwater flow systems, mostly concentrated in the permeable sediments and in the top 20 to 40 m of the fractured bedrock aquifer (Figures 25 to 27). Although the simulated local flow systems in the Appalachian Highlands extend in some areas down to 800 meters below the bedrock surface (Figure 25), the relative significance of the volume of flow decreases rapidly with depth. Local flow systems have a maximum horizontal scale of approximately 5 km with flow directions that tend to be parallel to the topography.

In this study, active flow is defined as being in those areas which receive more than an average groundwater flux of 1 mm/year. This limit is reached at a depth of approximately 30 m below the rock surface in the St. Lawrence Lowlands and approximately 60 m below the rock surface in the Appalachian Highlands (Figure 28). The difference in the depth of the active flow zone between these two geological provinces highlights the effects of topography and recharge on the shape of the flow systems.

Furthermore, the prominent topographic features of the Appalachian Highlands also generate an intermediate flow system originating from the highest topographic peaks to the south and emerging at the Appalachian foothills, spanning more than 20 km (Figures 23 and 24).

The model also confirms the existence, under the assumed simulated conditions, of a deep regional groundwater flow path emerging near the St. Lawrence River which would originate from the Appalachian Highlands (Figure 23). It is important to point out, however, that this regional system (defined between the two deepest streamlines in figure 25), containing only about 0.5 m^3/year per meter of transverse width, represents less than 0.005% of the total flow in the domain. Mean groundwater age simulations presented later in Section 3.4 also show that this deep flow would be extremely slow, with mean ages on the scale of geological time (tens of millions of years).

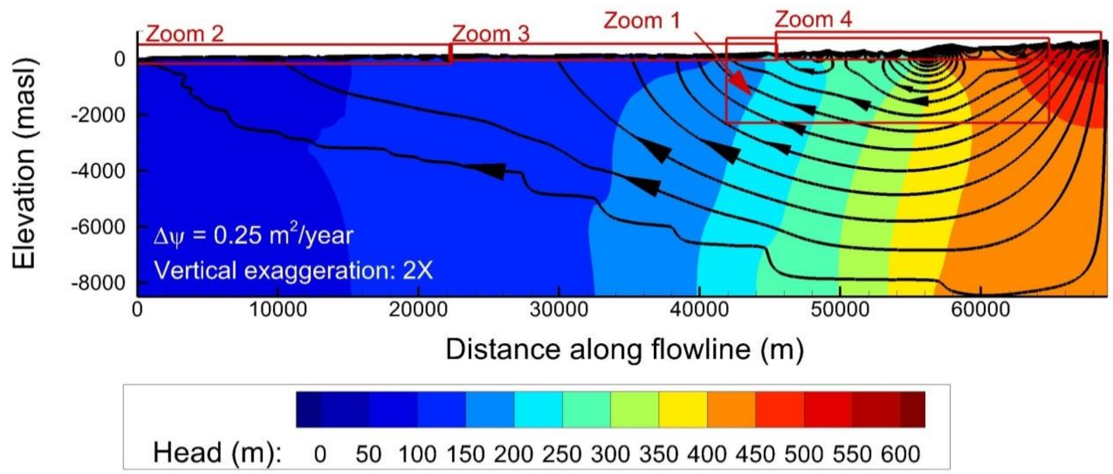

Figure 23 Calibrated steady-state flow model showing hydraulic heads and streamline distribution

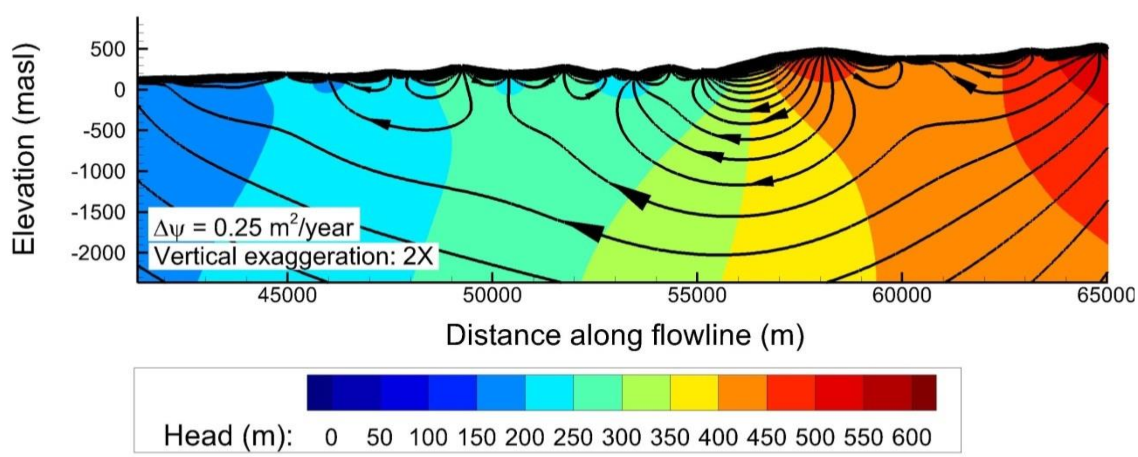

Figure 24 Calibrated flow model Zoom 1 (Appalachian Highlands): hydraulic heads and streamline distribution (location shown in Fig. 23).

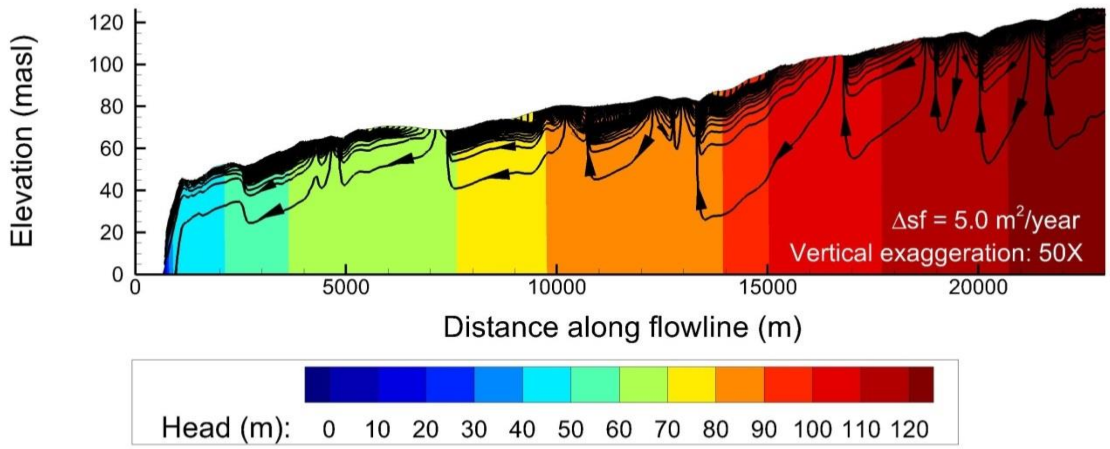

Figure 26 Calibrated flow model Zoom 2 (St. Lawrence Lowlands close to St. Lawrence River): hydraulic heads and streamline distribution (location shown in Fig. 23).

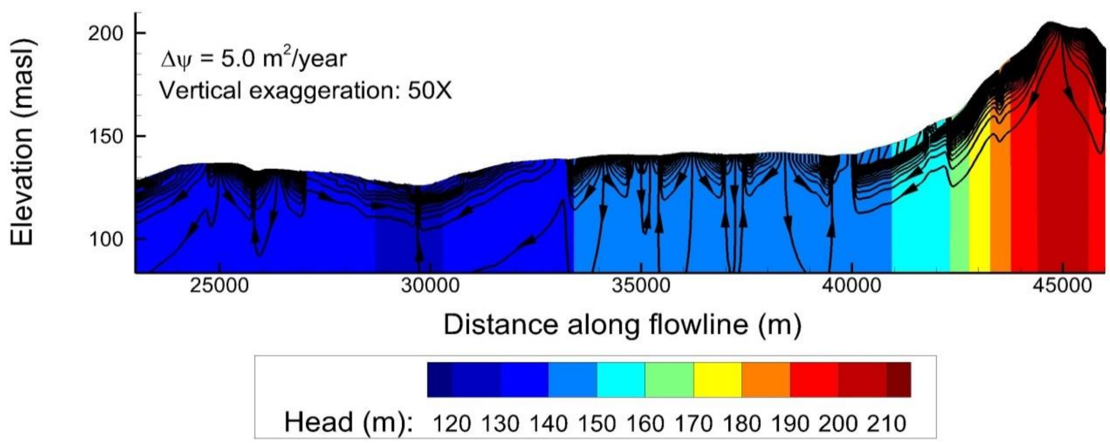

Figure 26 Calibrated flow model Zoom 3 (St. Lawrence Lowlands close to Appalachian front): hydraulic heads and streamline distribution (location shown in Fig. 23).

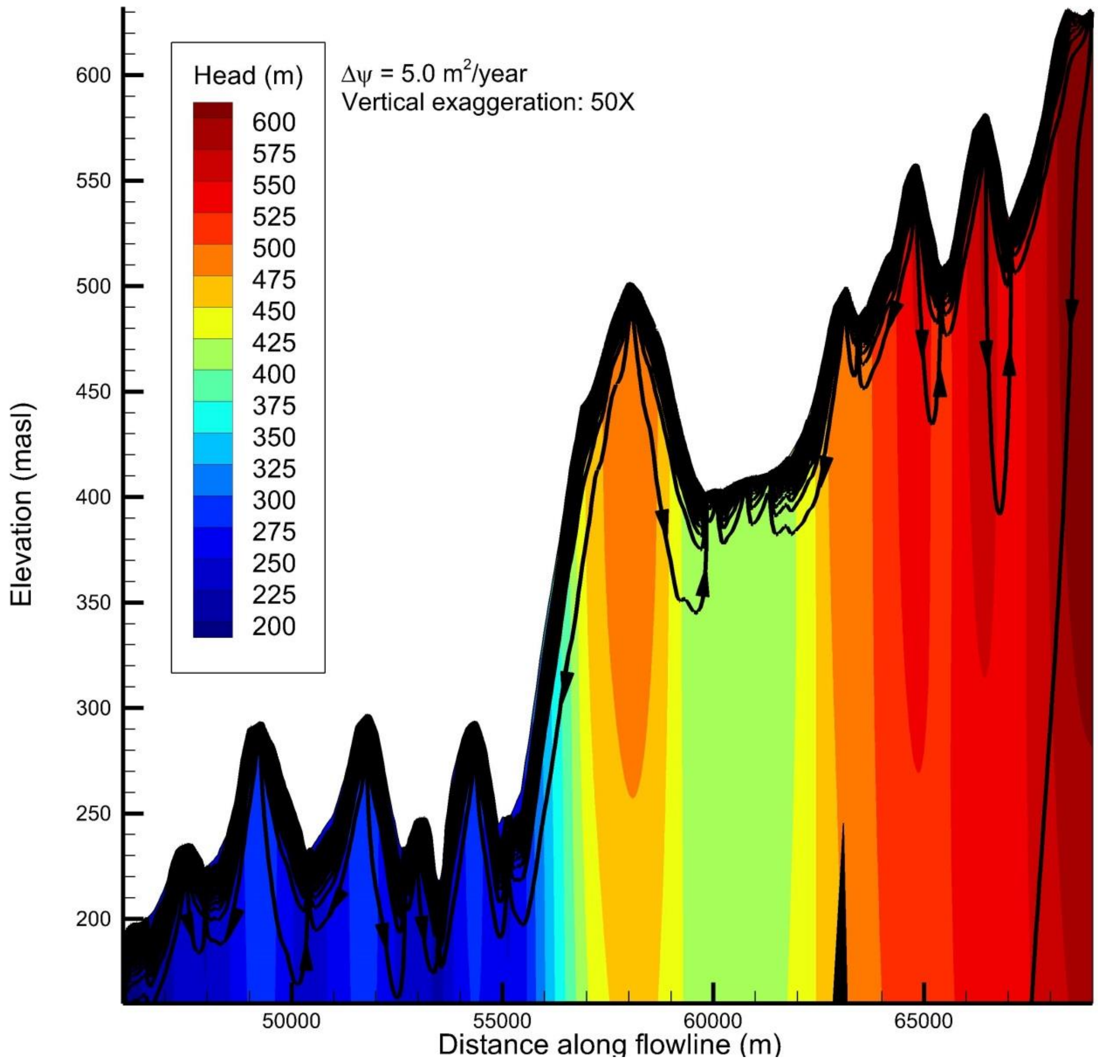

Figure 27 Calibrated flow model Zoom 4 (Appalachian Highlands): hydraulic heads and streamline distribution (location shown in Fig. 23).

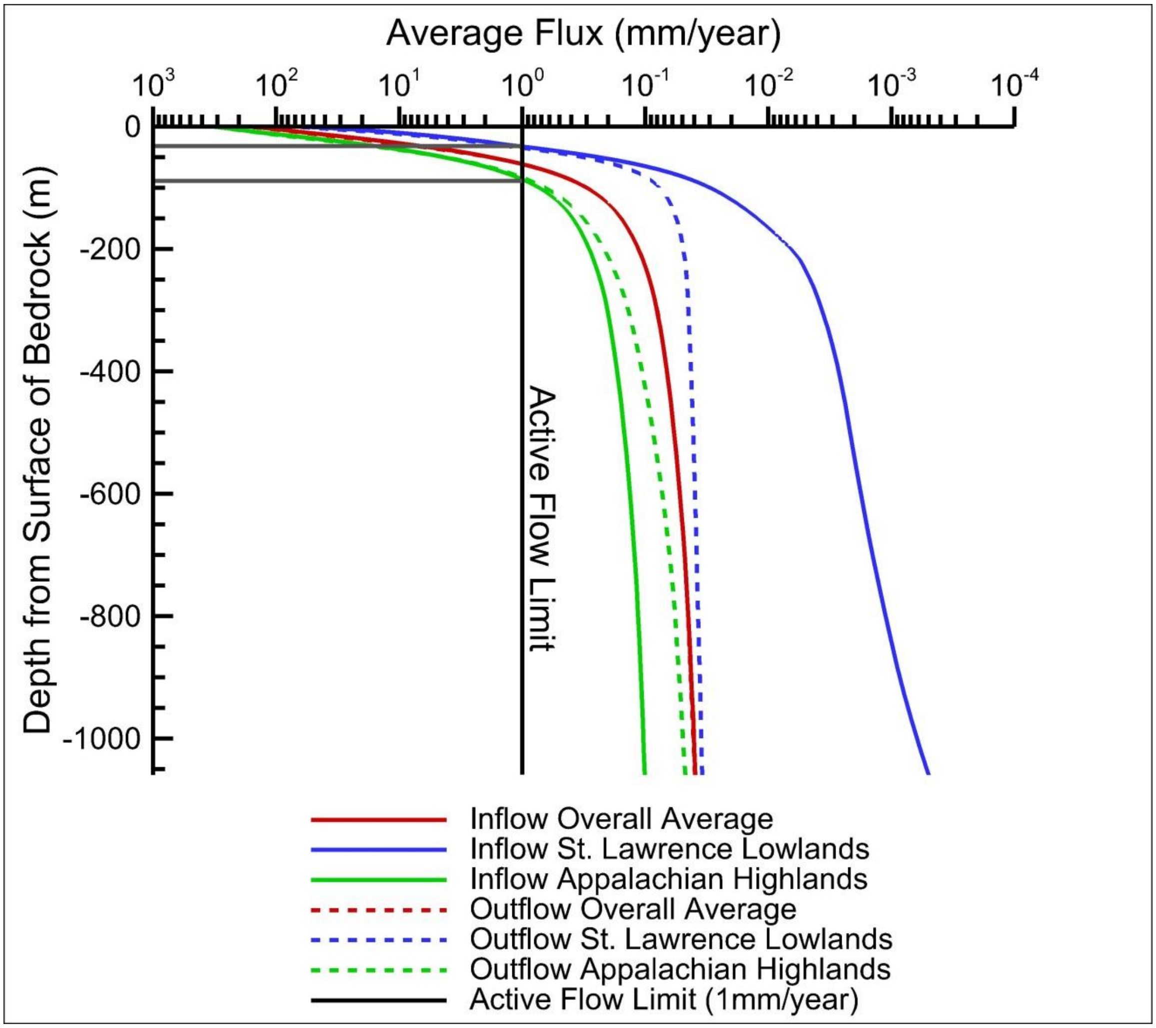

Figure 28 Average vertical Darcy fluxes as a function of depth from the surface of bedrock